Research Square

Preprints are preliminary reports that have not undergone peer review.
They should not be considered conclusive, used to inform clinical practice,
or referenced by the media as validated information.

Screening of ferroptosis-related prognostic genes of nasopharyngeal carcinoma and construction of prognosis prediction model

Liangliang Wang

wlljy80@163.com

Faculty of Chinese Medicine, Medical Science Division, Macau University of Science and Technology

Lili Yu

Faculty of Chinese Medicine, Medical Science Division, Macau University of Science and Technology

Qianghe Liu

Department of Otolaryngology-Head and Neck Surgery, The First Affiliated Hospital of Guilin Medical University

Fangxian Liu

Department of Otolaryngology-Head and Neck Surgery, The First Affiliated Hospital of Guilin Medical University

Feng He

Department of Otolaryngology-Head and Neck Surgery, The First Affiliated Hospital of Guilin Medical University

Jing Sun

Department of Intensive Care Medicine, Nanxishan Hospital

Research Article

Keywords: Nasopharyngeal Carcinoma, ferroptosis, bioinformatics analysis, prognostic model

Posted Date: September 3rd, 2026

DOI: https://doi.org/10.21203/rs.3.rs-10692162/v1

License: This work is licensed under a Creative Commons Attribution 4.0 International License.
Read Full License

Additional Declarations: No competing interests reported.

Abstract

Objective: This study aimed to utilize bioinformatics methods to identify ferroptosis-related genes associated with the prognosis of nasopharyngeal carcinoma (NPC) and to develop a prognostic prediction model for this cancer type.

Methods: The limma package identified differentially expressed genes (DEGs) between nasopharyngeal carcinoma (NPC) and normal tissues from the GSE12452 dataset. Ferroptosis-related genes were subsequently intersected with these identified DEGs to pinpoint differentially expressed ferroptosis-related genes. Univariate Cox regression analysis, in conjunction with LASSO regression, was then applied to the GSE10234 dataset to identify key prognostic risk genes and develop a prognostic assessment model for NPC. Univariate and multivariate Cox regression analyses were further performed to identify independent prognostic factors for NPC. Non-parametric tests were employed to evaluate the association between risk scores and clinical characteristics within distinct high- and low-risk groups. The clusterProfiler package was utilized for KEGG pathway enrichment analysis of DEGs comparing these risk groups. Finally, to corroborate these findings, the expression of the identified prognostic genes was compared between the human immortalized nasopharyngeal epithelial cell line NP69 and nasopharyngeal carcinoma cell lines to validate their differential expression patterns.

Results: A prognostic signature was constructed using GLS2, TFRC, and EPSA1. In vitro experiments confirmed high expression of GLS2 and TFRC in tumor cells, while EPSA1 exhibited low expression. Survival analysis and ROC curve assessments demonstrated the model's effectiveness in predicting NPC prognosis. Univariate and multivariate regression analyses subsequently revealed the risk score, derived from this signature, as an independent prognostic factor for NPC. Non-parametric tests indicated that this risk score was significantly associated ($P < 0.05$) with EB infection type, clinical stage, and morphological characteristics across high- and low-risk groups. Finally, KEGG pathway enrichment analysis showed that DEGs between these groups were predominantly enriched in pathways such as homologous recombination repair, ribosome signaling, DNA replication, hematopoietic cell regulation, T cell receptor signaling, and the lysosomal pathway.

Conclusion: This study identified three ferroptosis-related genes and constructed a prognostic model for NPC. This model can predict patient prognosis and guide personalized treatment plans.

INTRODUCTION

Nasopharyngeal carcinoma is a malignant epithelial tumor originating in the nasopharyngeal mucosa [1]. Its incidence shows significant regional variation, with notably higher rates observed in coastal areas of China, Southeast Asian countries, and northeastern Africa. Specifically, its incidence rate [2–4] is predominantly concentrated in China's Guangdong and Guangxi regions. In recent years, global morbidity and mortality rates associated with this cancer have shown a consistent upward trend [5]. These tumors are typically less differentiated and exhibit rapid progression. Due to the relatively concealed nature of

nasopharyngeal lesions, early clinical symptoms and signs tend to be subtle, making early detection challenging. Consequently, both distant metastasis and lymph node metastasis are common [6–7]. Most patients are diagnosed at advanced stages, often presenting with cranial nerve invasion, which results in a 5-year survival rate of less than 20% [8–9]. Therefore, there is an urgent need to identify accurate prognostic molecular markers and develop a prognostic prediction model for nasopharyngeal carcinoma to facilitate early assessment of patient prognosis.

Ferroptosis is a recently identified form of programmed cell death. Its primary characteristic is the iron-dependent accumulation of lipid peroxides in mitochondria, which ultimately leads to cell death [10–12]. This process operates through mechanisms significantly distinct from those of apoptosis, necroptosis, and pyroptosis [13–15]. Research has demonstrated that ferroptosis is regulated by diverse molecular mechanisms [16]. Current studies indicate that ferroptosis can be induced in both cancerous and certain normal cells through specific experimental compounds or clinical drugs, such as Erastin, Ras-selective lethal molecule 3 (RSL3), and sorafenib[17]. Notably, sorafenib is an anti-tumor agent approved by the U.S. Food and Drug Administration (FDA) for the treatment of various advanced cancers [18–21]. Furthermore, ferroptosis has been closely linked to several diseases, including Alzheimer's disease, acute kidney injury, myocardial ischemia-reperfusion injury, and glioma[22]. Previous studies have confirmed its significant role in head and neck squamous cell carcinoma [23–24], and numerous reports have highlighted the importance of ferroptosis-related genes (FRGs) in tumor prognosis [25–27]. However, the relationship between FRGs and the prognosis of patients with nasopharyngeal carcinoma remains to be elucidated. This study aims to investigate the expression and prognostic significance of FRGs in nasopharyngeal carcinoma, establish a prognostic prediction model based on their differential expression, and identify characteristic genes in clinical nasopharyngeal cancer specimens and adjacent paracancerous tissues. This research seeks to provide a foundation for personalized treatment and prognosis assessment for patients with nasopharyngeal cancer.

MATERIALS AND METHODS

1.1 Data Download and Processing

Nasopharyngeal cancer-related mRNA sequencing data and clinical information were downloaded from the GEO database (https://www.ncbi.nlm.nih.gov/geo/). Specifically, we utilized datasets GSE12452, GSE53819, and GSE102349. GSE12452 contained 31 nasopharyngeal cancer tissues and 10 control tissues, while GSE53819 comprised 18 nasopharyngeal cancer tissues and 18 control tissues. The GSE102349 dataset provided clinical metadata, including patient ID numbers, Epstein-Barr virus (EB) infection types, clinical stages, morphological characteristics, progression-free survival times, and survival statuses. For survival analysis, patients with missing progression-free survival data were excluded, resulting in a final cohort of 88 nasopharyngeal carcinoma patients. As GEO data are publicly available, this study was exempt from local ethics committee approval. Additionally, 259 ferroptosis-related genes were downloaded from the FerrDb database (http://www.zhounan.org/ferrdb).

1.2 Identification of Differentially Expressed Ferroptosis-Related Genes

Gene expression differences between nasopharyngeal cancer specimens and normal specimens were compared using the R language's limma package, applied to gene chip datasets GSE12452 and GSE53819. Common differentially expressed genes (DEGs) were identified by intersecting the results, applying a screening criterion of a corrected P-value of 1. These DEGs were then intersected with the previously downloaded ferroptosis-related genes to identify those specifically associated with nasopharyngeal cancer. Visualization of these differentially expressed ferroptosis-related genes will also be performed using R.

1.3 Identification of Risk-Related Ferroptosis Genes

LASSO regression combined with stepwise regression analysis will be used to identify risk genes. These risk genes will then be employed to construct a prognostic assessment model, defining the risk score (RS) as: $RS = \beta_1X1 + \beta_2X_2 + ... + \beta nXn$, where β represents the coefficients derived from multivariable regression analysis of the risk genes, and X denotes the relative expression levels of each gene. The risk score will be calculated for each sample using this formula. Samples will then be classified into high-risk or low-risk groups based on whether their risk score is above or below the median risk score, respectively. Survival curves and ROC curves will be utilized to evaluate the performance of the constructed model.

1.4 Assessment of Immune Infiltration Differences Between Risk Groups

The ssGSEA method will be employed to estimate the proportions of 28 common immune cells and immune functions in each sample. Non-parametric tests will then be applied to evaluate the associations between the identified risk groups, immune cell proportions, and immune functions. Additionally, the estimate package will be used to calculate the stromal score and immune score for each sample; these scores are expected to correlate closely with the risk coefficient. Finally, the distribution of signaling pathways and biological processes between the high-risk and low-risk groups will be discussed.

1.5 Identification of Independent Prognostic Risk Factors in Nasopharyngeal Cancer Patients

Clinical feature information from nasopharyngeal cancer patient files will be organized and integrated with the risk factors identified by the previously developed prognostic model. A Cox multifactor regression analysis will then be conducted using the R 'survival' package. This analysis will include generating forest plots to identify independent risk factors significantly influencing the prognosis of nasopharyngeal cancer.

1.6 Relationship Between Risk Score and Basic Clinical Characteristics of Nasopharyngeal Cancer Patients

Utilizing the risk scores derived from each sample, this section analyzes the relationship between these scores and various factors, including EB infection type, clinical stage, and histomorphological characteristics.

1.7 Cell line culture

The NPC cell lines (CNE-1, CNE-2, and C666-1) and the human immortalized nasopharyngeal epithelial cell line (NP69) were obtained from the Scientific Experimental Center of Guilin Medical University (Guilin, China). The cells were maintained in high-glucose DMEM media (Solarbio, Beijing, China) supplemented with 10% fetal bovine serum (Sijiqing Biotech, Hangzhou, China) and 1% penicillin-streptomycin solution (Solarbio, Beijing, China) in a 37°C, 5% CO_2 incubator (Thermo Fisher Scientific, USA).

1.8 Real-time quantitative polymerase chain reaction

Real-time quantitative PCR (RT-qPCR) was performed using the SYBR Green method. Total RNA was extracted using the TRIzol method (Vazyme). RNA concentration was measured using a NanoDrop-2000 spectrophotometer (Thermo Fisher Scientific, Inc.) and subsequently reverse transcribed using a FastQuant RT Super mix kit (Tiangen Biotech, Co, Ltd.). qPCR was performed using SYBR-Green qPCR Master Mix (Bimake Biotechnology) under the following thermal cycle conditions: initial denaturation at 95°C for 10 min, followed by 40 cycles of 95°C for 10 s, 60°C for 15 s, and 72°C for 30 s. Data were quantified using the 2^{-DDCT} method, with GAPDH used as an internal control to normalize target gene expression. The PCR primers used were as follows:

EPAS1-F TCAGAAAACATCAGCAAGT

EPAS1-R AGGTTCTCACGAATCTCC

GLS2-F CTGGGGAACAGCCATAGG

GLS2-R ACGCCGTGGGTCTAACTT

TFRC-F GAGACTTCTTCCGTGCTA

TFRC-R GAGACTCTTTTGGAGATACG

GPX4-F ATTCCCGAGCCTTTCAACCC

GPX4-R TATCGGGCATGCAGATCGAC

hGAPDH-F ATCCCATCACCATCTTCCAGG

hGAPDH-R CCATCACGCCACAGTTTCC

1.9 Western Blot

Proteins were separated by 10% SDS-PAGE and transferred to a polyvinylidene difluoride (PVDF) membrane (MilliporeSigma). The membranes were then incubated overnight with primary antibodies against EPAS1 (1:2000; Rabbit polyclonal, Catalog number 26422-1-AP, Wuhan Sanying), GLS2 (1:2000; Rabbit polyclonal, Catalog number 20171-1-AP, Wuhan Sanying), TFRC (1:5000; Rabbit polyclonal, Catalog number 10084-2-AP, Wuhan Sanying), and GAPDH antibody (rabbit monoclonal, [Catalog number 60004-1-Ig, Wuhan Sanying], diluted 1:5000). After being washed with PBS-Tween20 (1:500), membranes were incubated with the corresponding secondary antibody (1:5000; Wuhan Sanying) for 60 minutes. Protein bands were visualized using an enhanced chemiluminescence detection kit (Beyotime). Images were captured using a chemiluminescence imaging system (Shanghai Qinxian ChemiScope 6200Touch) and analyzed with ImageJ (National Institutes of Health, Bethesda, Maryland, USA).

1.10 Statistical Analysis

Statistical analyses were performed using R version 4.0.2, which also facilitated graph generation. The rank-sum test was employed to compare the expression levels of ferroptosis-related genes between nasopharyngeal cancer and normal tissues. Cox regression analysis was used to construct a multigene prognostic risk model. Survival and ROC curves were generated to assess the model's clinical detection capability. Differences in risk scores among subgroups were evaluated using nonparametric tests.

RESULTS

2.1 Screening for differentially expressed ferroptosis genes in different tissues

Public and clinical data for datasets GSE12452, GSE53819, and GSE102349 were downloaded from the GEO database. Concurrently, 259 ferroptosis-related genes were obtained from the FerrDb database. Specifically, GSE12452 contained 31 nasopharyngeal cancer (NPC) samples and 10 normal samples, GSE53819 included 18 NPC samples and 18 normal samples, and GSE102349 provided 113 NPC samples with corresponding follow-up data. Principal Component Analysis (PCA) was conducted to illustrate the differences between tumor and normal tissue samples (Fig. 1A). The genes DEGs were identified separately in GSE12452 and GSE53819, yielding an intersection of 406 genes. These 406 DEGs were then intersected with the 259 ferroptosis-related genes, leading to the identification of 8 differentially expressed ferroptosis-related genes (Fig. 1B). These genes were further visualized using a Venn diagram (Fig. 1C) and a volcano plot (Fig. 1D).

2.2 Construction of a Prognostic Risk Model for Ferroptosis-Related Genes in Nasopharyngeal Carcinoma

To identify ferroptosis-related genes significantly associated with nasopharyngeal carcinoma (NPC) prognosis, LASSO regression analysis was performed on the 8 identified ferroptosis genes (Fig. 2A). This analysis identified four ferroptosis genes—EPAS1, GLS2, IL33, and TFRC—as significantly related to NPC occurrence and progression. Subsequently, stepwise regression further refined the selection to three ferroptosis-related genes (EPAS1, GLS2, and TFRC) for constructing a prognostic prediction model for NPC. The calculation formula for the risk model is: risk value (RS) = GLS2 × 0.5850393 - EPAS1 × 0.5591266 + TFRC × 0.5143543 (Fig. 2B).

2.3 Validation of Ferroptosis-Related Genes and the Prognostic Model in Nasopharyngeal Carcinoma

Patients were stratified into high- and low-risk groups based on their calculated risk scores. Analysis of these groups revealed that the progression-free survival rate in the high-risk group was significantly lower than that in the low-risk group ($P < 0.01$) (Fig. 2C). To further validate the prognostic model's accuracy, ROC curves were generated using the R "survival ROC" package for 1-, 3-, and 5 year survival predictions (Fig. 2D). The model demonstrated strong predictive ability, with AUCs of 0.81, 0.75, and 0.78 for 1-, 3-, and 5-year survival, respectively, confirming its capability in predicting NPC patient prognosis.

2.4 Relationship Between High- and Low-Risk Groups and Immune Infiltration

Gene Set Enrichment Analysis (GSEA) revealed significant differences in the expression of most immune cells between the high-risk and low-risk groups (Fig. 3A). These differences were also notably associated with common immune functions (Fig. 3B) and variations in tumor stroma and immune scores (Fig. 3C). Subsequently, Gene Set Variation Analysis (GSVA), utilizing the limma package, was performed to investigate differences in signaling pathways (Fig. 4A) and variations in shear enrichment biological processes between the two groups (Fig. 4B). These analyses suggested a relationship with microsatellite instability pathways.

2.5 Risk factors affecting the prognosis of nasopharyngeal cancer.

Univariate and multivariate regression analyses (Fig. 5A, Fig. 5B) revealed that only the risk coefficient significantly influenced progression-free survival in patients with nasopharyngeal cancer. Additionally, the univariate analysis identified Epstein-Barr virus type as being associated with progression-free survival in these patients.

2.6 Risk coefficient and clinical correlation with nasopharyngeal cancer.

Non-parametric test results indicated that various types of EB virus infections and different tissue morphology types in the high- and low-risk groups were significantly associated with the risk coefficient (Fig. 5C, Fig. 5E, $P < 0.05$). Although the small number of stage I and II cases precluded a calculation of differences between these two groups, notable differences in risk coefficients were still observed between the high- and low-risk groups in stages III and IV (Fig. 5D, $P < 0.05$).

2.7 Expression analysis of prognostic genes in cell lines

The expression of three prognostic genes was verified by RT-qPCR in NPC cell lines. The RT-qPCR results for the three prognostic genes in NPC cell lines (C666-1, CNE-2, and CNE-1) and the human immortalized nasopharyngeal epithelial cell line (NP69) were consistent with the previously observed expression differences (Figs. 6A–C).

Protein expression levels of TFRC, EPAS1, and GLS2 were further validated by western blotting in cell lines. Western blot confirmed that the protein level of EPAS1 was decreased in NPC cell lines (C666-1, CNE-2, and CNE-1) compared with that in the human immortalized nasopharyngeal epithelial cell line (NP69). Similarly, the protein levels of TFRC and GLS2 were also significantly decreased compared with those in NP69 (Figs. 6D-F). Therefore, TFRC, EPAS1, and GLS2 not only possess prognostic value for NPC patients but are also expected to become potential therapeutic targets for NPC in the future.

DISCUSSION

Recent studies indicate that ferroptosis can either inhibit or promote tumor progression by releasing signaling molecules within the tumor microenvironment[28]. Additionally, siderophils may influence tumor progression through chemotaxis or interactions with immune cells, regulating anti-tumor immune responses [29––33]. Furthermore, certain genes implicated in Head and Neck Squamous Cell Carcinoma (HNSCC) are involved in drug-induced ferroptosis. Recent research has identified ferritin-related genes that are closely associated with the overall survival rate of HNSCC patients[34]. However, the relationship between these genes and the overall survival rate of nasopharyngeal cancer (NPC) patients remains unclear. NPC is a malignant tumor highly prevalent in southern regions of my country. Although early-stage NPC has a high cure rate, the survival rate for patients with intermediate and advanced tumors remains low despite comprehensive treatment. Prognosis is influenced by factors such as the extent of tumor infiltration, lymph node metastasis, distant metastasis, and treatment duration. Nevertheless, the absence of effective biomarkers poses a significant challenge in the diagnosis and prognosis assessment of early-stage NPC. Therefore, identifying reliable molecular markers for predicting nasopharyngeal carcinoma prognosis, along with developing prognostic prediction biological models, is crucial for guiding patient outcomes.

Ferroptosis is a newly identified form of programmed cell death, and its potential involvement in both normal physiological processes and disease development, similar to apoptosis and autophagy, is an active area of research. The crucial role of iron in tumor cell death has been extensively reported[35–36].

Abnormal iron metabolism and accumulation in cells and mitochondria can accelerate tumor growth and contribute to malignancy[37]. Significantly, even when tumor cells evade other forms of cell death, they often remain sensitive to ferroptosis[38], offering a theoretical basis for its investigation in cancer[39]. Our study analyzed nasopharyngeal cancer and normal tissue samples from the GEO database, identifying 25 differentially expressed ferroptosis-related genes. Univariate regression analysis further revealed three genes significantly associated with nasopharyngeal cancer survival: TFRC, GLS2, and EPAS1. Among these, ferritin-related genes, exemplified by the transferrin receptor (TFRC), showed an independent association with survival. The transferrin receptor (TFRC) is a crucial protein for iron transport and metabolism in the body. Beyond its role in iron homeostasis, TFRC also mediates cell growth, proliferation, and metabolism. Its overexpression has been shown to significantly diminish c-Myc-induced tumor formation [40].

In contrast, mitochondrial glutaminase (GSL2), a downstream target of p53, is the key enzyme converting glutamine to glutamate. GLS2 expression increases in a p53-dependent manner, particularly following DNA damage or oxidative stress, due to p53 association with its promoter. Studies show that GLS2 overexpression inhibits tumor cell growth and colony formation[41]. EPAS1 (Endothelial PAS Domain Protein 1 (EPAS1) is a crucial transcription factor enabling cells to respond to hypoxia. While predominantly expressed in umbilical vascular endothelial cells, EPAS1 mRNA expression notably increases under intracellular hypoxic conditions. Tumor cells are highly responsive to hypoxia, and research indicates EPAS1 enhances tumor vasculature by regulating downstream genes, thereby accelerating cancer cell proliferation and inhibiting apoptosis[42–43].

In light of these findings, we constructed a prognostic model using these ferroptosis-related genes. We calculated a risk score (RS) and analyzed its relationship with survival outcomes in high- and low-risk groups. To assess the model's accuracy and clinical relevance, ROC curves were generated for 1, 3, and 5 years, with AUC values used for evaluation. With all AUC values exceeding 70%, the results suggest that this risk assessment model effectively predicts the prognosis of patients with nasopharyngeal cancer.

Several factors, including age, tumor grade, and stage, influence the prognosis of patients with NPC. Early studies identified the Epstein-Barr virus (EBV) in the serum of NPC patients. Later, PCR technology detected the EBV genome directly in tumor cells, further solidifying its association with NPC. Recent technological advancements have shown EBV to be present in nearly all non-keratinizing NPC tumor cells, a unique finding as it is rarely detected in other head and neck tumors, thus confirming its distinct correlation with NPC [44]. The expression of specific EBV genes may indicate recurrence in advanced NPC, suggesting their potential as prognostic indicators for advanced cases[45–46]. Our univariate analysis identified EBV subtypes (EB_type) and risk models. When all identified risk factors were integrated into a multifactorial regression analysis, only the risk coefficient emerged as a significant determinant of progression-free survival in NPC patients. Further non-parametric tests indicated that this risk coefficient was associated with the tissue's EB type and correlated with clinical stage, thereby

reaffirming the stability of our risk assessment model for NPC. We speculate that this model, based on its determined AUC values, could offer clinicians a reliable prognostic assessment tool.

This study has certain limitations. The ferroptosis-related gene model, established using the GEO database, requires further validation with regional clinical data. Future research will utilize a new dataset for a more in-depth analysis to identify 'ferroptosis core genes' closely associated with NPC prognosis and to explore their relationships with multiple signaling pathways.

In summary, this study constructed a novel prognostic model comprising three ferroptosis-related genes independently associated with overall survival. This model offers insights into predicting NPC patient prognosis and provides clinicians with a theoretical foundation for personalized treatment strategies.

Declarations

Conflict of Interest: The authors declare no conflict of interest.

Availability of data and materials

The results shown here are in whole or part based upon data generated by TCGA (https://www.cancer.gov/tcga), KEGG (https://www.genome.jp/kegg), GO (http://geneontology.org), GEO (https://www.ncbi.nlm.nih.gov/geo).

Ethical approval

The nasopharyngeal carcinoma cell lines were kindly provided by the Central Laboratory of Guilin Medical University. Because no human subjects or animal experiments were directly involved in this study. Therefore, no additional ethical approval was required.

Consent to participate

For the bioinformatics analysis, all datasets used are publicly available and de-identified, so informed consent was not applicable. For the cell experiment part, no human participants were involved.

Consent to publish

All authors consent to publication. The study did not include identifiable individual data or clinical images requiring specific consent.

Author Contributions

Lianglinag Wang conceived and designed the study. Qianghe Liu and Fangxian Liu performed the bioinformatics analysis, including data acquisition from TCGA/GEO, prognostic model construction, and statistical analysis. Jing Sun conducted the qPCR and western blot experiments. Lili Yu revised the manuscript. All authors reviewed and approved the final version.

Acknowledgements

The authors thank The Cancer Genome Atlas (TCGA) and Gene Expression Omnibus (GEO) for providing publicly available data. We are grateful to the Central Laboratory of Guilin Medical University for generously providing the nasopharyngeal carcinoma cell lines used in this study. This work was supported by Guangxi Medical and Health Appropriate Technology Research and Development (Project Contract Number: S201316-01); Self-funded Research Project of Guangxi Health Commission (Z-C20250776)

Data availability

The study was performed based on the TCGA and GEO public databases. The datasets generated and/or analyzed during this study are available in the following public repositories:

(1) TCGA data: https://portal.gdc.cancer.gov/; (2) GEO dataset GSE12452: https://ftp.ncbi.nlm.nih.gov/geo/series/GSE12nnn/GSE12452/matrix/; (3) GEO dataset GSE53819: https://ftp.ncbi.nlm.nih.gov/geo/series/GSE53nnn/GSE53819/matrix/; (4) GEO dataset GSE102349: https://www.ncbi.nlm.nih.gov/geo/query/acc.cgi;

Competing interests

The authors declare that the research was conducted in the absence of any commercial or financial relationships that could be construed as a potential conflict of interest.

References

1. Li J-Y, Xiao T, Yi H-M, Yi H, Feng J, Zhu J-F, et al. S897 phosphorylation of EphA2 is indispensable for EphA2-dependent nasopharyngeal carcinoma cell invasion, metastasis and stem properties. Cancer Lett. 2019;444:162–74.
2. Zhu J-F, Huang W, Yi H-M, Xiao T, Li J-Y, Feng J, et al. Annexin A1-suppressed autophagy promotes nasopharyngeal carcinoma cell invasion and metastasis by PI3K/AKT signaling activation. Cell Death Dis. 2018;9:1154.
3. Chen J. Lu F,Hu C,MicroRNA-299 targets VEGFA and inhibits the growth,chemosensitivity and invasion of human nasopharyngeal carcinoma cells[J]. J BUON. 2019;24(5):2049–55.
4. Chen W, Zheng R, Zhang S et al. Annual report on status of cancer in China,2010.[J].Chinese Journal of Cancer Research. 2014,26(1):48–58.
5. Chua MLK, .Wee JTS, Hui EP, Chan ATC. Nasopharyngeal carcinoma. Lancet. 2016;387:1012–24.
6. Zeng G-Q, Yi H, Li X-H, Shi H-Y, Li C, Li M-Y, et al. Identification of the proteins related to p53-mediated radioresponse in nasopharyngeal carcinoma by proteomic analysis. J Proteom. 2011;74:2723–33.

7. Zheng Z. MiR-125b regulates proliferation and apoptosis of nasopharyngeal carcinoma by targeting A20/NF-κB signaling pathway. Cell Death Dis. 2017;8:e2855.
8. Lee AWM, Lin JC, Ng WT. Current management of nasopharyngeal cancer. Semin Radiat Oncol. 2012;22:233–44.
9. Lee AWM, Ma BBY, Ng WT, Chan ATC. Management of nasopharyngeal carcinoma: current practice and future perspective. J Clin Oncol. 2015;33:3356–64.
10. Ivana Čepelak S, Dodig. Daniela Čepelak Dodig. Ferroptosis:regulated cell death [J]. Arh Hig Rada Toksikol. 2020;71(2):99–109.
11. Stockwell BR, Friedmann Angeli JP, Bayir H, Bush AI, Conrad M, Dixon SJ, Fulda S, Gascon S, Hatzios SK, Kagan VE, et al. Ferroptosis: a regulated cell death nexus linking metabolism, redox biology, and disease. Cell. 2017;171(2):273–85.
12. Shen Z, Song J, Yung BC, Zhou Z, Wu A, Chen X. Emerging strategies of cancer therapy based on ferroptosis. Adv Mater. 2018;30(12):e1704007.
13. Dixon SJ. Lemberg KM,Lamprecht MR,Skouta R,Zaitsev EM,Gleason CE,Patel DN,Bauer AJ,Cantley AM,Yang WS,et al.Ferroptosis:an iron dependent form of nonapototic cell death. Cell. 2012;149(5):1060–72.
14. Yang WS, et al. Regulation of ferroptotic cancer cell death by GPX4. Cell. 2014;156(1–2):317–31.
15. JIANG X, STOCKWELL B R CONRADM, Ferroptosis. mecha□nisms, biology and role in disease[J]. Nat Rev Mol Cell Biol. 2021;22(4):266–82.
16. Hirschhorn T, Stockwell BR. The development of the concept of ferroptosis. Free Radic Biol Med. 2019;133:130–43.
17. Xie Y, Hou W, Song X, Yu Y, Huang J, Sun X, Kang R, Tang D. Ferroptosis: process and function. Cell Death Difer. 2016;23(3):369–79.
18. Cabanillas ME, Ryder M, Jimenez C. Targeted therapy for advanced thyroid cancer: kinase inhibitors and beyond. Endocr Rev. 2019;40(6):1573–604.
19. Llovet JM. Montal R,Sia D,Finn RS.Molecular therapies and precision medicine for hepatocellular carcinoma. Nat Rev Clin Oncol. 2018;15(10):599–616.
20. Escudier B, Eisen T, Stadler WM, Szczylik C, Oudard S, Siebels M, Negrier S, Chevreau C, Solska E, Desai AA, et al. Sorafenib in advanced clear-cell renal-cell carcinoma. N Engl J Med. 2007;356(2):125–34.
21. Abdelgalil AA, Alkahtani HM, Al-Jenoobi FI. Sorafenib Profles Drug Subst Excip Relat Methodol. 2019;44:239–66.
22. Wang Y, Wei Z,Pan K, et al. The function and meichism of ferroptsis in cancer [. J] Apoptosis. 2020;25(11/12):786–98.
23. Lee J, You JH, Shin D, Roh JL. Inhibition of glutaredoxin 5 predisposes cisplatin-resistant head and neck cancer cells to ferroptosis. Theranostics. 2020;10(17):7775–86.

24. Shin D, Lee J, You JH, Kim D, Roh JL. Dihydrolipoamide dehydro-genase regulates cystine deprivation-induced ferroptosis in head and neck cancer. Redox Biol. 2020;30:101418.
25. Han F, Li W, Chen T, et al. Ferroptosis-related genes for predicting prognosis of patients with laryngeal squamous cell carcinoma. Eur Arch Otorhinolaryngol. 2021;278:2919–25.
26. Jiang P, Yang F, Zou C, Bao T, Wu M, Yang D, Bu S. The construction and analysis of a ferroptosis-related gene prognostic signature for pancreatic cancer. Aging. 2021;13(Apr4):10396–414.
27. Zhu L, Yang F, Wang L, Dong L, Huang Z, Wang G, Chen G, Li Q. Identifcation the ferroptosis-related gene signature in patients with esophageal adenocarcinoma. Cancer Cell Int. 2021;21(1):124.
28. Li SC, Xuan YP, Gao B, et al. Identification of an eight gene prognostic signature for lung adenocarcinoma. Cancer Manaq Res. 2018;10:33383–3392.
29. Wang W, Green M, Choi JE, Gijon M, Kennedy PD, Johnson JK, Liao P, Lang X, Kryczek I, Sell A, et al. CD8(+)Tcells regulate tumour ferroptosis during cancer immunotherapy. Nature. 2019;569(7755):270–4.
30. Sun Y, Chen P, Zhai B, Zhang M, Xiang Y, Fang J, Xu S, Gao Y, Chen X, Sui X, et al. The emerging role of ferroptosis in infammation. Biomed Pharmacother. 2020;127:110108.
31. Rothe T, Gruber F, Uderhardt S, Ipseiz N, Rossner S, Oskolkova O, Bluml S, Leitinger N, Bicker W, Bochkov VN, et al. 12/15-Lipoxygenase-mediated enzymatic lipid oxidation regulates DC maturation and function. J Clin Invest. 2015;125(5):1944–54.
32. Angeli JPF, Krysko DV, Conrad M. Ferroptosis at the crossroads of cancer-acquired drug resistance and immune evasion. Nat Rev Cancer. 2019;19(7):405–14.
33. Kloditz K, Fadeel B. Three cell deaths and a funeral: macrophage clearance of cells undergoing distinct modes of cell death. Cell Death Discov. 2019;5:65.
34. Qun L, Yang LJ, et al. Construction of a Ferroptosis-Related Gene Signature for Head and Neck Squamous Cell Carcinoma Prognosis Prediction [J]. Int J Gen Med. 2021;14:10117–29.
35. CONRAD M,LORENZS M,PRONETH B. Targeting ferroptosis:new hope for as-yet-incurable disease [J]. Trends Mol Med. 2020;27(2):113–22.
36. ELGENDY S M, ALYAMMAHI S K,ALHAMAD D W, et al. Ferroptosis: an emerging approach for targeting cancer stem cells and drug resistance [J]. Crit Rev Oncol Hematol. 2020;155:103095.
37. YU M, GAI C, LI Z, et al. Targeted exosome-encapsulated erastin induced ferroptosis in triple negative breast cancer cells[J]. Cancer Sci. 2019;110(10):3173–82.
38. Bebber CM, Muller F, Prieto Clemente L, Weber J, von Karstedt S. Ferroptosis in cancer cell biology. Cancers. 2020;12(1):164.
39. Mou Y, Wang J, Wu J, et al. Ferroptosis, a new form of cell death: opportunities and challenges in cancer. J Hematol Oncol. 2019;12(1):34.
40. Wang H, Yang B,Geng T, et al. Tissue-specifics election of optimal reference genes for expression analysis of anti-cancer drug-related genes in tumors amples using quantitative real-time RT-PCR[J]. Exp Mol Pathol. 2015;98(3):375–81.

41. Sawako Suzuki T, Tanaka MV, Poyurovsky, et al. Phosphate-activated glutaminase (GLS2), a p53-inducible regulator of glutamine metabolism andreactive oxygen species [. J] PNAS. 2010;107(16):7461–6.
42. Keith B, Johnson RS, Simon MC. HIF1 and HIF2: sibling rivalry in hypoxic tumour growth and progression [J]. Nat Rev Cancer. 2011;12(1):9–22.
43. Courtnry KD, Infante JR, Lam ET, Phase I, et al. Dose-Escalation Trial of PT2385,a First-in-Class Hypoxia-Inducible-Factor-2 Antagonist in Patients With Previously Treated Advanced Clear Cell Renal Cell Carcinoma[J]. J Clin Oncol. 2018;36(9):867–74.
44. Young LS. Dawson CW.Epstein-Barr virus and nasopharyngeal carcinoma [. J] Chin J Cancer. 2014;33(12):581–90.
45. Chan AT, Nasopharyngeal carcinoma, Ann. Oncol. 21 (, Liu F et al. Biomedicine & Pharmacotherapy. 2019;120:1095335.
46. Fung SY, Lam JW, Chan KC. Clinical utility of circulating Epstein-Barr virus DNA analysis for the management of nasopharyngeal carcinoma. Chin Clin Oncol. 2016;5(2):18.

Figures

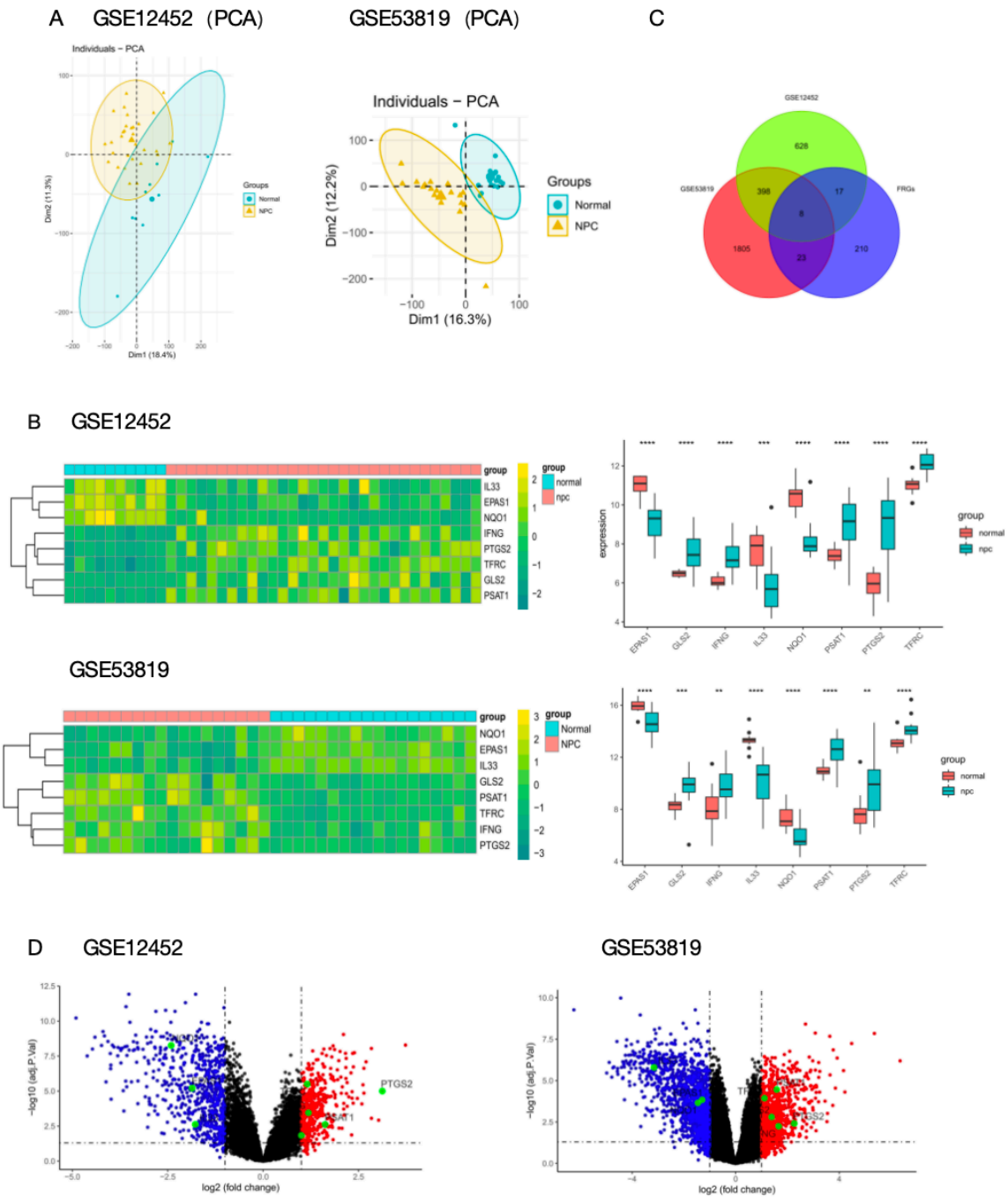


FIGURE 1 | (A) PCA analysis of nasopharyngeal carcinoma (NPC) and normal tissue. (B) Ferroptosis-related genes and their expression in nasopharyngeal carcinoma from datasets GSE12452 and GSE53819. (C) Visualization of differential genes using a Venn diagram. (D) Visualization of the volcano plot for differential genes.

Figure 1

See image above for figure legend.

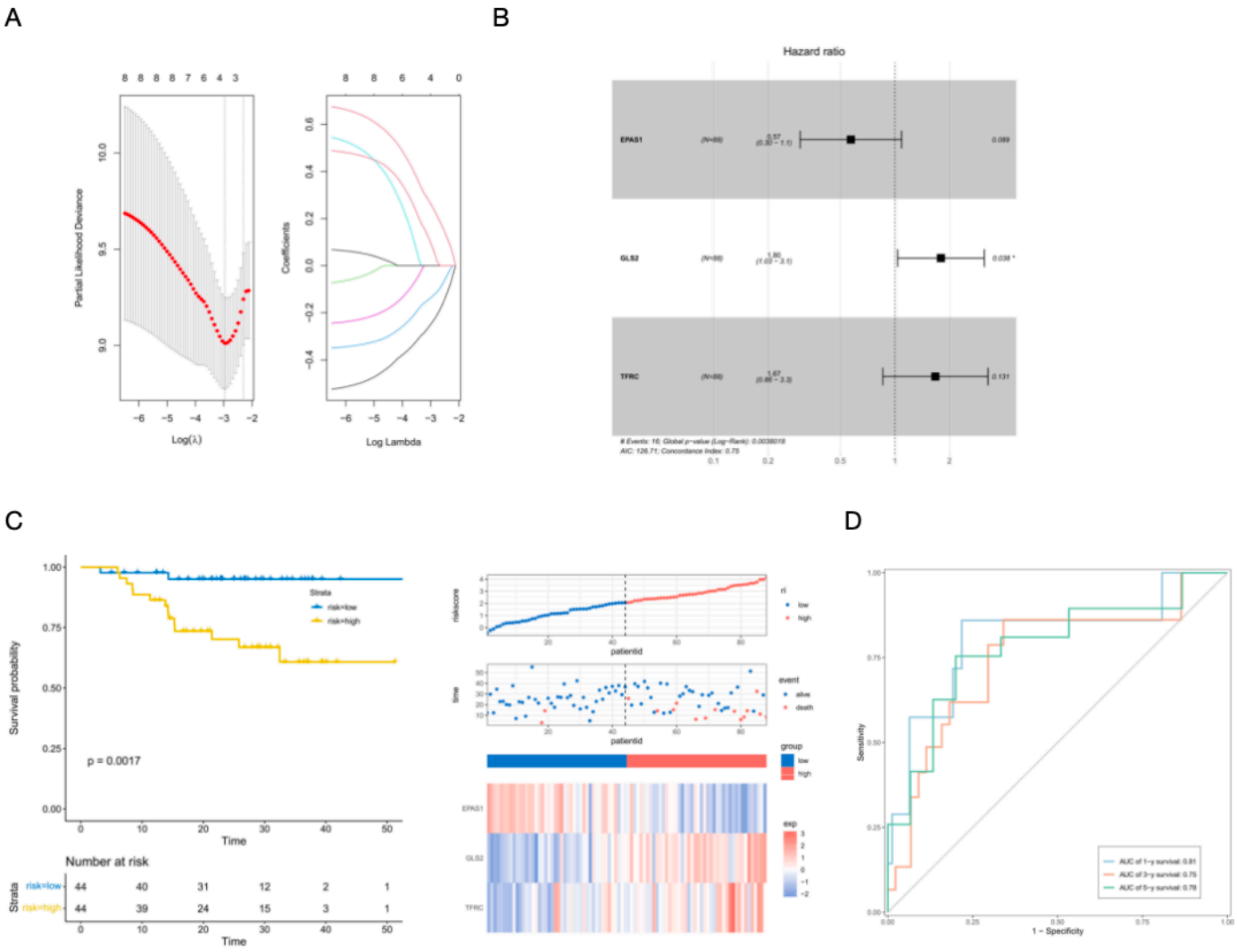


FIGURE 2 | (A) LASSO regression analysis of differential ferroptosis genes associated with nasopharyngeal cancer. (B) Construction of a risk model based on the risk ratios of three ferroptosis-related genes. (C) Analysis of the relationship between risk values and survival outcomes in high and low-risk groups. (D) Receiver Operating Characteristic (ROC) curves for 1, 3, and 5 years.

Figure 2

See image above for figure legend.

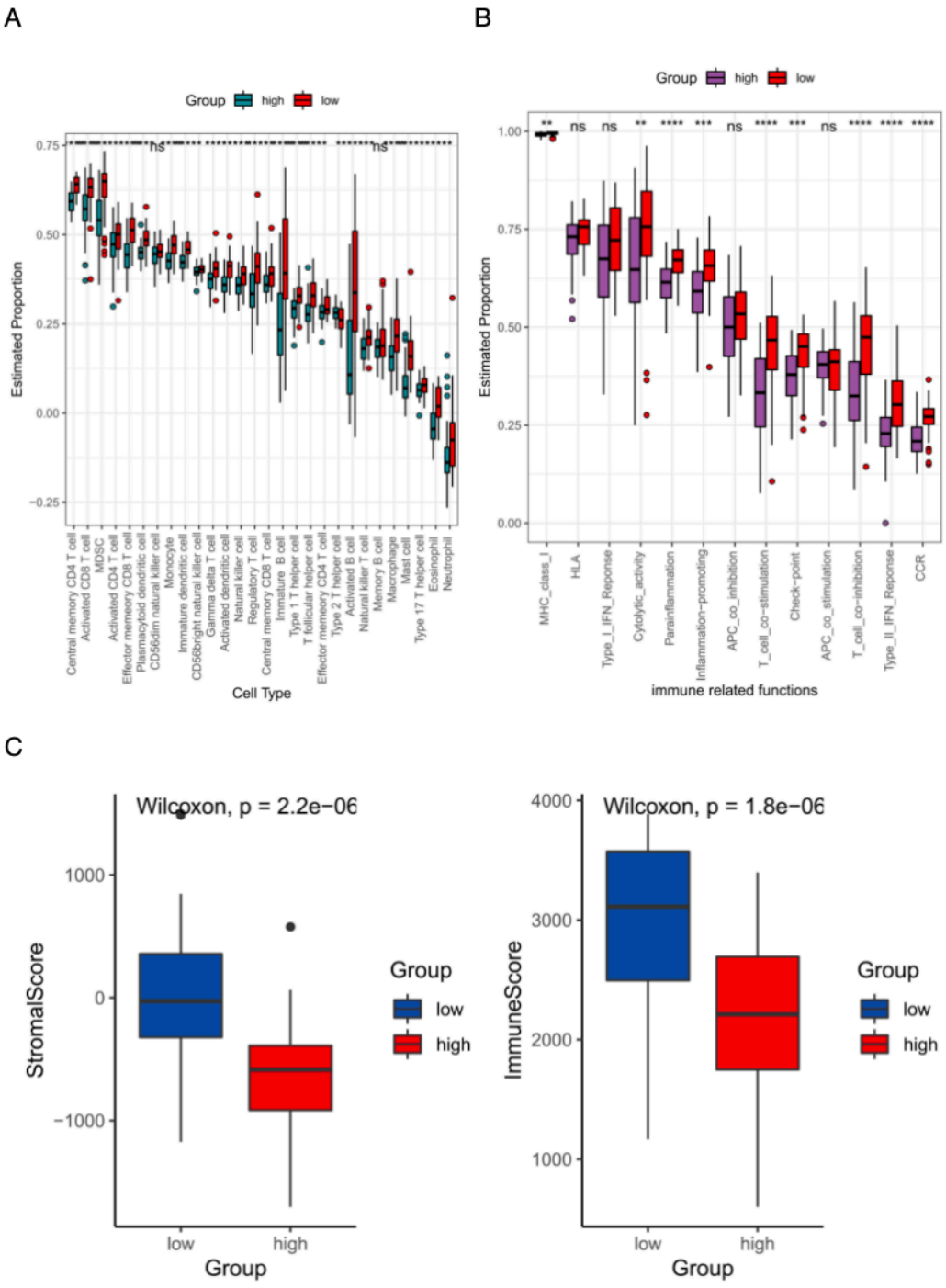


FIGURE 3 | (A) Differences in immune cell expression between high- and low-risk groups. (B) Correlation of common immune functions between high- and low-risk groups. (C) Correlation between tumor stromal score and immune score in high- and low-risk groups.

Figure 3

See image above for figure legend.

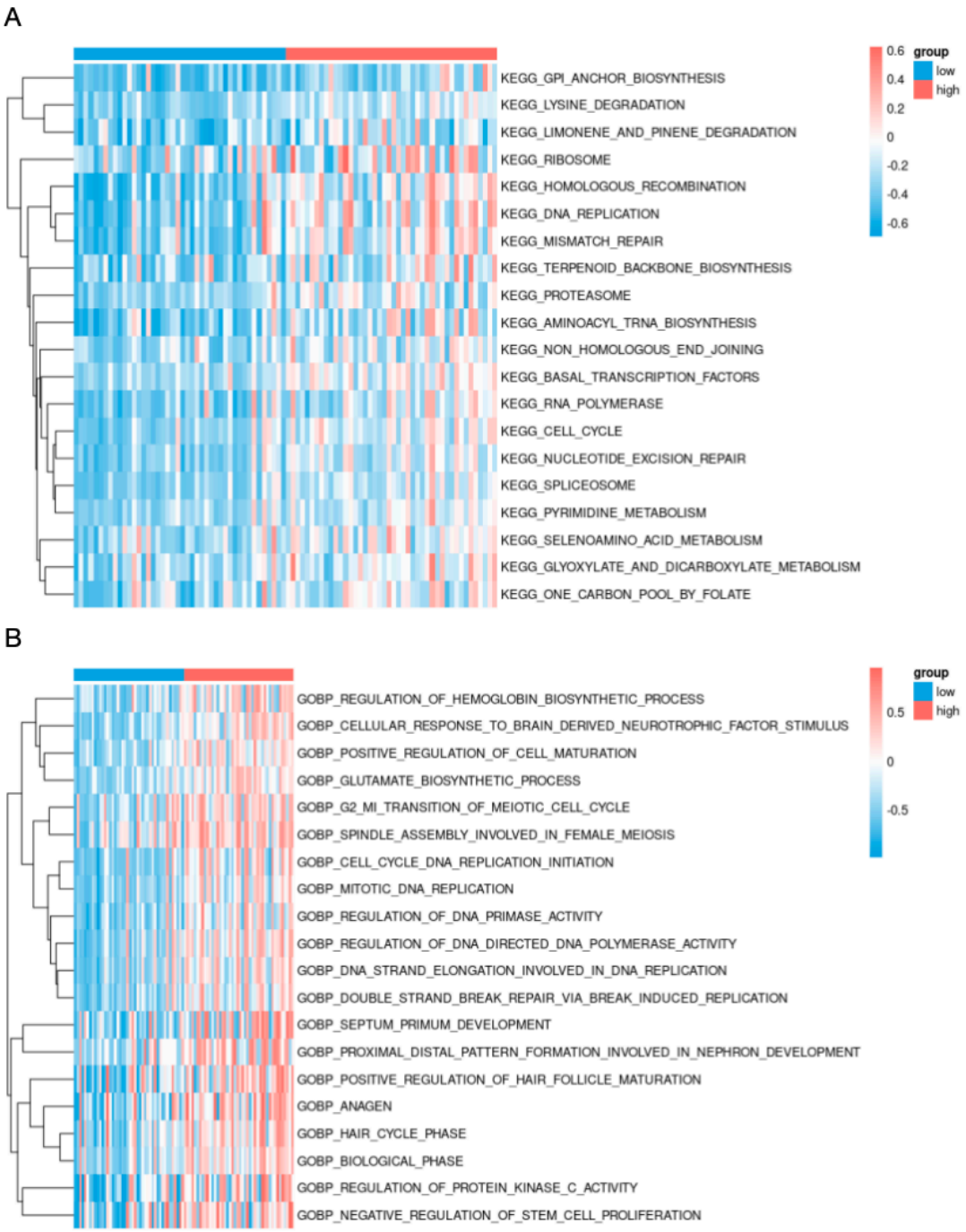


FIGURE 4 | (A) Differences in signaling pathways between high- and low-risk groups. (B) Variations in biological processes associated with shear enrichment between high-risk and low-risk groups.

Figure 4

See image above for figure legend.

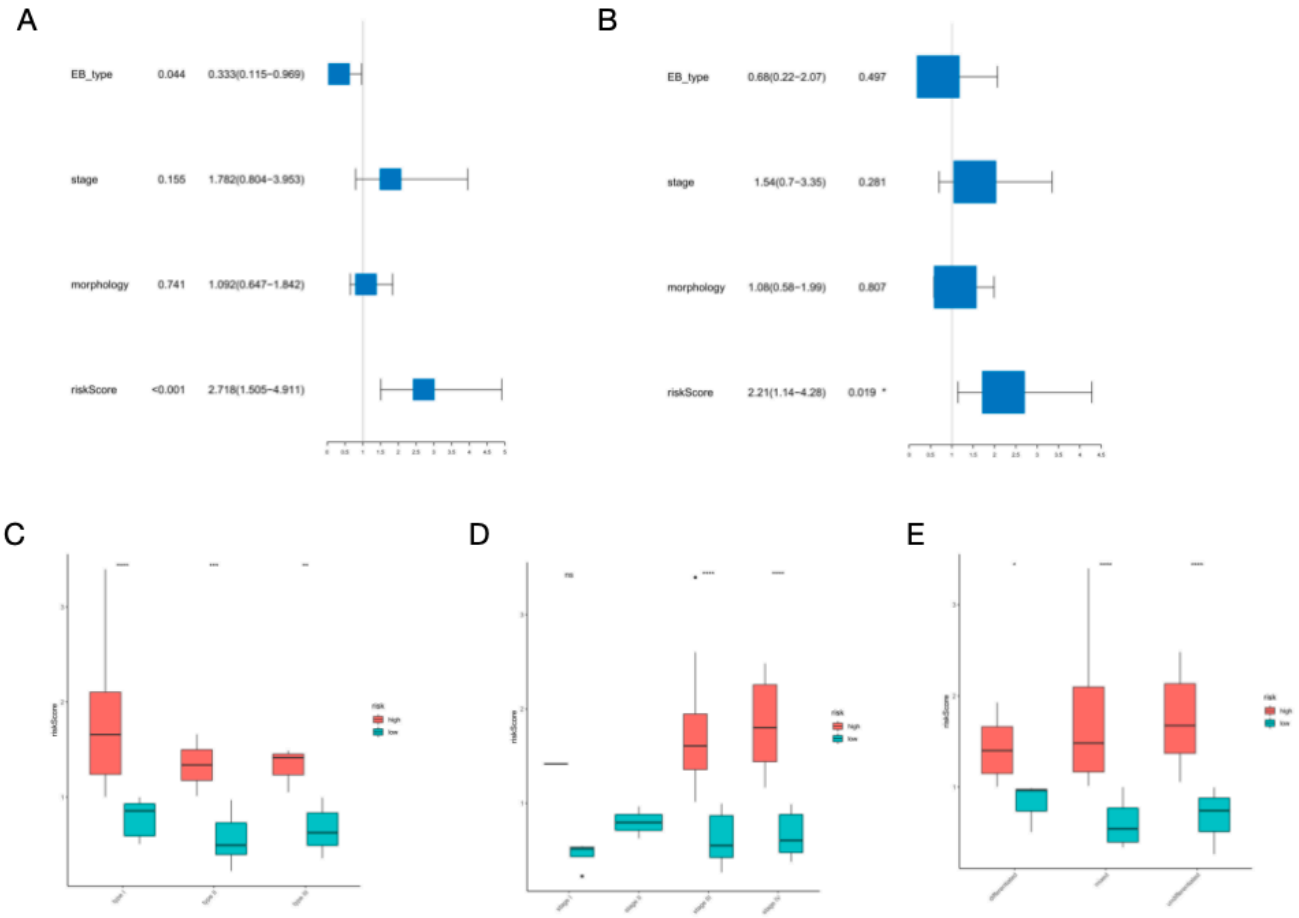


FIGURE 5 | (A) Single-factor regression analysis. (B) Multi-factor regression analysis. (C) The relationship between the type of EB virus infection and the risk coefficient. (D) The relationship between clinical stage and the risk coefficient. (E) The relationship between tissue morphology and the risk coefficient.

Figure 5

See image above for figure legend.

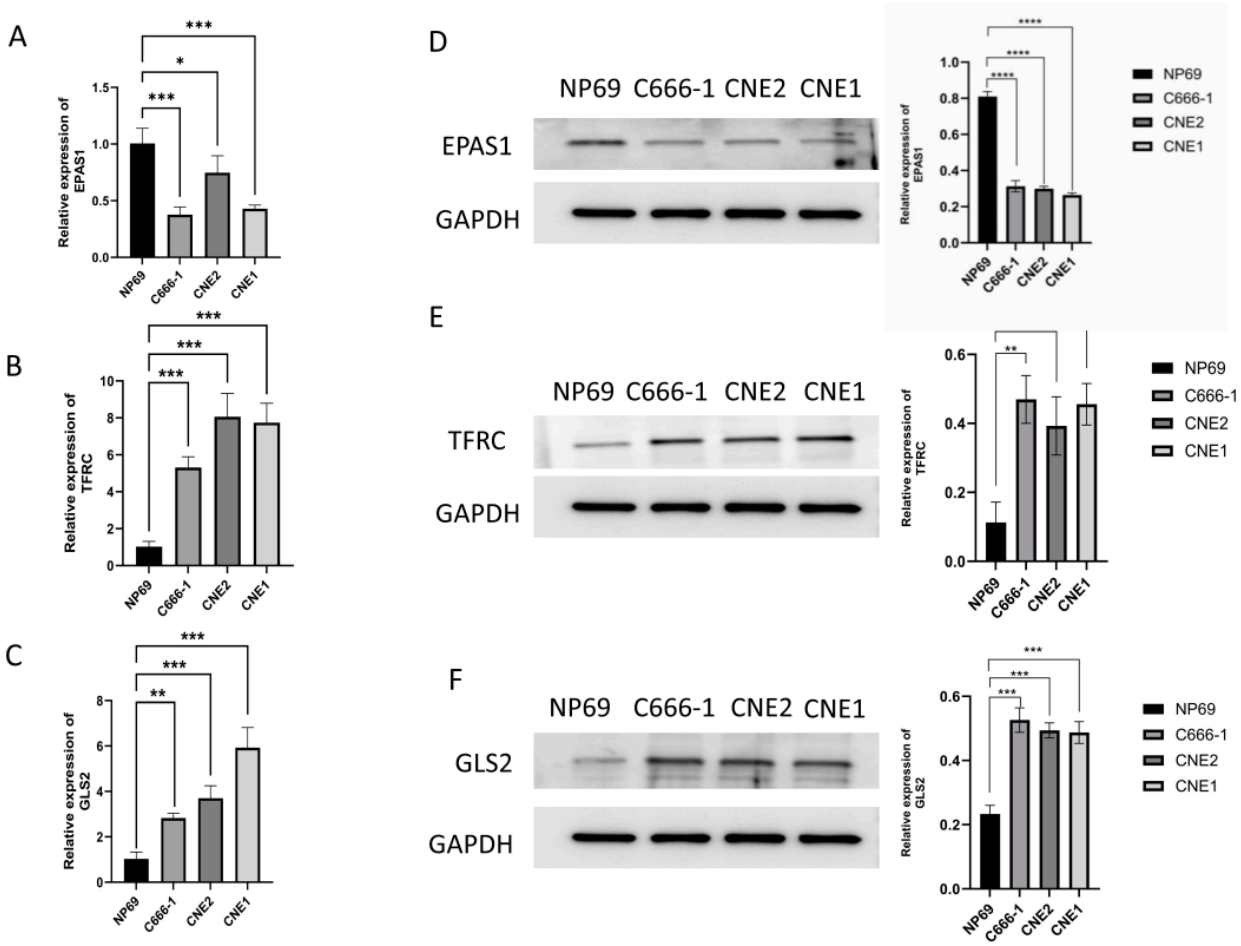


Figure6|(A-C)Expression analysis of the three genes between normal cell line and Nasopharyngeal Cancer cell lines.(D) the protein level of EPAS1 was decreased in NPC cell lines compared with that in nomal cell line.(E-F) the protein level of TFRC and GLS2 was significantly decreased compare with innomal cell line.

Figure 6

See image above for figure legend.

Supplementary Files

This is a list of supplementary files associated with this preprint. Click to download.

- Westernblot.7z